

# POLARIZATION PATTERN OF FRESHWATER HABITATS RECORDED BY VIDEO POLARIMETRY IN RED, GREEN AND BLUE SPECTRAL RANGES AND ITS RELEVANCE FOR WATER DETECTION BY AQUATIC INSECTS

GÁBOR HORVÁTH\* AND DEZSÖ VARJÚ†

*Lehrstuhl für Biokybernetik, Universität Tübingen, Auf der Morgenstelle 28, D-72076 Tübingen, Germany*

*Accepted 30 January 1997*

## Summary

The reflection-polarization patterns of small freshwater habitats under clear skies can be recorded by video polarimetry in the red, green and blue ranges of the spectrum. In this paper, the simple technique of rotating-analyzer video polarimetry is described and its advantages and disadvantages are discussed. It is shown that the polarization patterns of small water bodies are very variable in the different spectral ranges depending on the illumination conditions. Under clear skies and in the visible range of the spectrum, flat water surfaces reflecting light from the sky are most strongly polarized in the blue range. Under an overcast sky radiating diffuse white light, small freshwater habitats are characterized by a high level of horizontal polarization at or near the Brewster angle in all spectral ranges except that in which the contribution of subsurface reflection is large. In a given spectral range and at a given angle of view, the direction of polarization is

horizontal if the light mirrored from the surface dominates and vertical if the light returning from the subsurface regions dominates. The greater the degree of dominance, the higher the net degree of polarization, the theoretical maximum value being 100 % at the Brewster angle for the horizontal E-vector component and approximately 30 % at flat viewing angles for the vertical E-vector component. We have made video polarimetric measurements of differently coloured fruits and vegetables to demonstrate that polarized light in nature follows this general rule. The consequences of the reflection-polarization patterns of small bodies of water for water detection by polarization-sensitive aquatic insects are discussed.

Key words: rotating-analyzer video polarimetry, polarization patterns, colour, polarization, freshwater habitats, visual ecology, polarization sensitivity, aquatic insects, water detection.

## Introduction

Recently, Schwind (1991, 1995) has demonstrated that many insects living in or on, or visiting, water recognize their aquatic habitat by the horizontal polarization of reflected light. The sensitivity maxima of their polarization vision are in various spectral regions between the ultraviolet ( $\lambda < 360$  nm) and the yellowish-green ( $\lambda \approx 550$  nm). The habitat choice of these insects might be affected by the very variable reflection-polarization characteristics of natural bodies of water. As Schwind pointed out, the degree of polarization of aquatic habitats can vary widely because of the light reflecting back from the water itself: 'When diffuse subsurface reflection makes a large contribution in a particular spectral region, the polarization in that region, which depends on light reflected from the surface, can be greatly reduced or even abolished' (p. 439 in Schwind, 1995).

The primary aim of this work is to illustrate this thesis of

Schwind by visualizing the reflection-polarization patterns of two typical freshwater habitats over a relatively wide field of view. Although Schwind quantified the degree of polarization of light reflected at the Brewster angle from a dark pond and a bright eutrophic body of water as a function of wavelength (see Fig. 8A in Schwind, 1995), there was no technique available to make similar measurements in a wider field of view. We have used rotating-analyzer video polarimetry to measure the reflection-polarization characteristics of small freshwater habitats under clear skies in the red, green and blue ranges of the spectrum. We visualized the brightness, degree and direction of polarization in two-dimensional false-colour maps with pixel resolution. The biological relevance of these reflection-polarization patterns for polarization vision in aquatic insects is discussed. The second goal of this work is to describe our simple rotating-analyzer video polarimetric

\*Permanent address: Biophysics Group, Department of Atomic Physics, Loránd Eötvös University, H-1088 Budapest, Puskin u. 5–7, Hungary (e-mail: gh@hercules.elte.hu).

†Author for correspondence (e-mail: dezsoe.varju@uni-tuebingen.de).

method and to discuss its advantages and disadvantages. Our technique is a low-cost and simplified version of the imaging polarized light analyzer developed by Wolff (1993).

### Materials and methods

The four main steps of video polarimetry are illustrated in Fig. 1. We first filmed the selected scene with a video camera recorder (CCD-VX1E Sony video Hi8 handycam) through a common linearly polarizing filter (Melles Griot, mounted dichroic sheet polarizer) in front of the objective lens. To avoid any translation or rotation, the camera was fixed to a horizontal holding plateau set up on a tripod (Fig. 1A). This holding plateau was pitched only to the degree required by the object being filmed, but was not rolled. Prior to recording, the automatic adjustment mode of the camera was switched off,

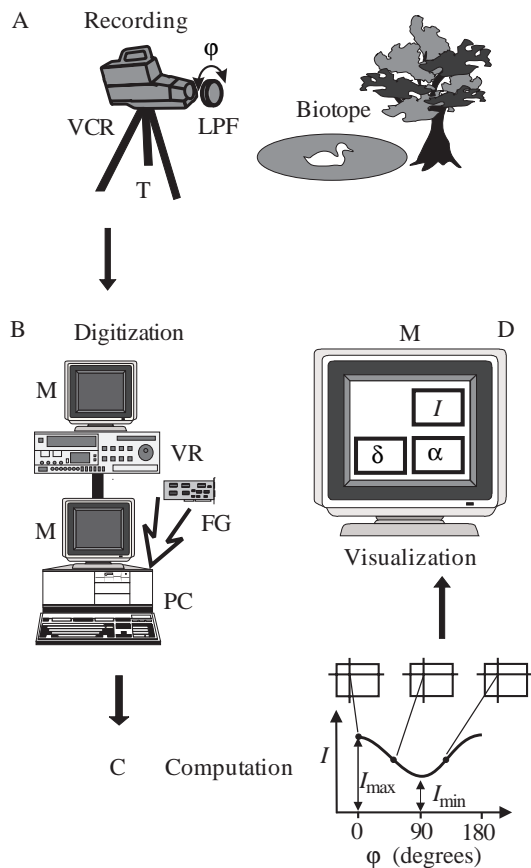


Fig. 1. Schematic representation of the technique of rotating-analyzer video polarimetry. (A) Recording using a video camera mounted with a rotating linearly polarizing filter in front of the objective lens. (B) Digitizing the recorded pictures using a frame grabber in a personal computer connected directly to the video camera recorder or to a video recorder. (C) Evaluating the brightness (or light intensity), the degree and the direction of polarization of the recorded scene on the basis of the brightness modulation from pixel to pixel. (D) Visualizing the patterns of the brightness  $I$ , the degree  $\delta$  and the direction  $\alpha$  of polarization on the computer screen. LPF, linear polarizing filter; VCR, video camera recorder; T, tripod; PC, personal computer; FG, frame grabber; VR, video recorder; M, monitor;  $\phi$ , alignment of polarizer.

the focus, aperture, shutter speed and gain were then manually selected and the settings of these parameters were locked. During recording, the polarizer was manually turned in  $45^\circ$  steps. The initial alignment of the direction of polarization of the filter was vertical. After a few seconds, it was turned twice by  $45^\circ$ ; thus, its final direction became horizontal. The direction of the filter was acoustically coded: the value of the angle was spoken into the built-in microphone and was recorded as an audio signal.

Further steps in the procedure were performed in the laboratory (Fig. 1B–D). The recorded scenes were digitized frame by frame using a frame grabber (Screen Machine II, FAST Multimedia AG, Munich) in a personal computer (IBM PC/486) connected directly to the handycam used in the field or to a stop-frame video recorder (Fig. 1B). From three digitized video pictures taken with the three different alignments ( $\phi=0^\circ$ ,  $45^\circ$  and  $90^\circ$ ) of the polarizer, we obtained the modulation of the brightness (or light intensity)  $I$  as a function of  $\phi$ . A sinusoid ( $I=A\sin\phi+B$ ) was fitted to this brightness modulation for each pixel of the picture (Fig. 1C). Although the brightness of partially polarized light viewed through a linearly polarizing filter varies as  $\sin^2\phi$ , it is sufficient to use  $\sin\phi$  in order to determine  $I_{\max}$ ,  $I_{\min}$  and the angular position  $\alpha$  of  $I_{\max}$ . From these parameters, we calculated the mean light intensity,  $I=(I_{\max}+I_{\min})/2$ , and the degree of polarization,  $\delta=(I_{\max}-I_{\min})/(I_{\max}+I_{\min})$ , for every point in the image. Finally, we produced a two-dimensional colour map of the brightness, degree and direction of polarization on the computer screen with pixel resolution (Fig. 1D). An accurate name for this procedure would be ‘computer-aided, wide-field-of-view, rotating-analyzer video polarimetry’, but we have shortened this to ‘video polarimetry’ in the rest of this paper. It is a wide-field polarimetry because the field of view is limited only by the field of view of the camera (with our camcorder, the maximum was approximately  $50^\circ$  in the horizontal direction and  $40^\circ$  in the vertical direction), which is much wider than that of conventional polarimeters (Azzam and Bashara, 1989; Collett, 1994).

In our CCD-VX1E video camera recorder, a picture is processed in three colour channels, red (R,  $\lambda_{\max}=730$  nm), green (G,  $\lambda_{\max}=600$  nm) and blue (B,  $\lambda_{\max}=470$  nm) to give  $3\times 3$  pictures of the scene filmed: the two-dimensional patterns of the brightness, degree and direction of polarization measured in the R, G and B spectral ranges. The brightness patterns are shaded in colours R, G and B, while the patterns of the degree and direction of polarization are displayed in false colours.

The digitized response of the single pixels of the video chip is approximately a linear function of brightness when light intensities are not too high. In order to remain in this linear region, we always selected an appropriate set of values of the aperture, shutter speed and gain, a procedure that requires a relatively high level of experience and skill.

### Results

To demonstrate the power of video polarimetry and to illustrate the effect of colour on the polarization of objects, we

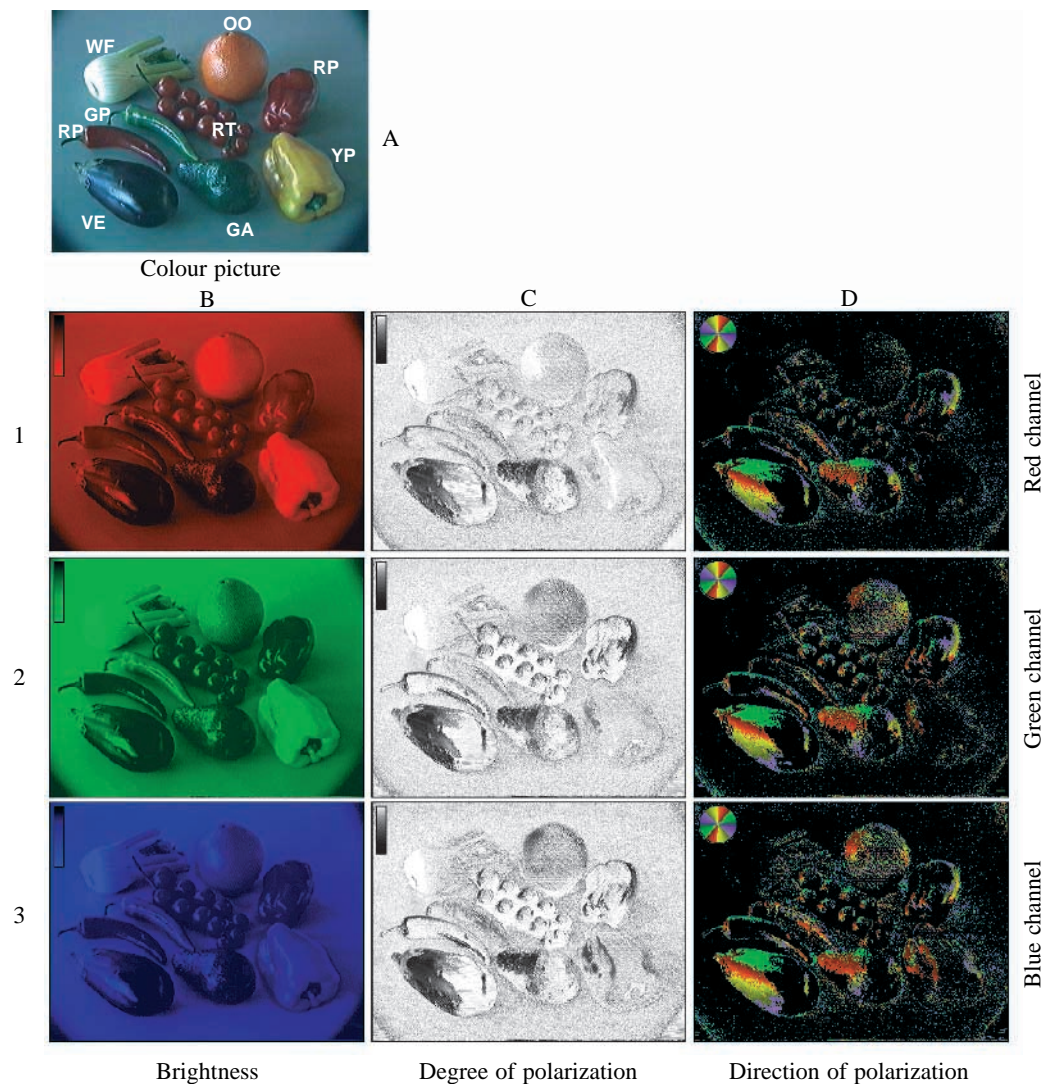
first examined the polarization patterns of differently coloured natural objects. The colour picture as seen through the camera is shown in Fig. 2A. The distributions of the brightness, degree and direction of polarization of a collection of fruits and vegetables measured by video polarimetry through the red, green and blue channels of the camera are shown in Fig. 2B–D. We chose this collection because it enables us to illustrate several general rules of reflection polarization of non-metallic objects at the same time; that is, the effect of surface roughness, curvature and colour. The collection was set up on the horizontal plane of a table and illuminated through a window by the unpolarized light from an overcast sky and by unpolarized room lights. The scene was filmed by the camera at an angle of view of  $50^\circ$  to the vertical.

The surfaces of the white fennel (WF) and ochre orange (OO) were relatively rough and, therefore, the degree of polarization of reflected light is weaker than that reflected from other fruits and vegetables with a smooth, shiny surface (see column C in Fig. 2). Rough surfaces reflect light diffusely, which reduces polarization. Since the reflected light becomes

partially polarized parallel to the reflector, the E-vector always follows the curvature of the surface. This can be seen in column D of Fig. 2, where the E-vector maps of the collection are presented.

More remarkable is the influence of colour on the degree of polarization of reflected light. In column B of Fig. 2, the brightness of white (fennel), red (tomato, paprika, pepper), yellow (paprika), green (pepper, avocado) and violet (eggplant) objects in the red, green and blue channels are illustrated. In this brightness map, the red tomato, paprika and pepper are, of course, brightest when viewed through the red channel (Fig. 2B1). The same is true for the ochre orange, which contains a relatively large amount of red pigment. These reddish fruits and vegetables are darker when viewed through the green channel (Fig. 2B2) and darker still in the blue channel (Fig. 2B3). Their average degree of polarization, however, is lowest in the red channel and highest in the blue one, as demonstrated in column C of Fig. 2. A similar relationship is true for the green pepper and avocado: they are brightest and the reflected light is least polarized in the green

Fig. 2. (A) Colour picture of a collection of fruits and vegetables of different colours as seen through the camera. (B–D) The brightness (light intensity)  $I$  (column B), degree  $\delta$  (column C) and direction  $\alpha$  (column D) of the polarization pattern of the collection measured by video polarimetry through the red (row 1), green (row 2) and blue (row 3) channels of the camera. The different numerical values of  $I$ ,  $\delta$  and  $\alpha$  are coded by different colour tones: (i) the higher the brightness, the brighter is the red, green and blue tone (black,  $I=0$ ; brightest,  $I=255$ ); (ii) the higher the degree of polarization, the darker is the grey shade (white,  $\delta=0\%$ ; black,  $\delta=100\%$ ); (iii) the darker the red, green, violet and yellow colour, the more the direction of polarization deviates from the vertical (red,  $0^\circ \leq \alpha < 45^\circ$ ; green,  $45^\circ \leq \alpha < 90^\circ$ ; violet,  $90^\circ \leq \alpha < 135^\circ$ ; yellow,  $135^\circ \leq \alpha < 180^\circ$ ). In column D, black represents low degrees of polarization ( $\delta < 15\%$ ) at which point the term ‘direction of polarization’ loses its meaning. WF, white fennel root; OO, ochre orange; RT, red tomato; RP, red paprika and red pepper; YP, yellow paprika; GP, green pepper; GA, green avocado; VE, violet eggplant.



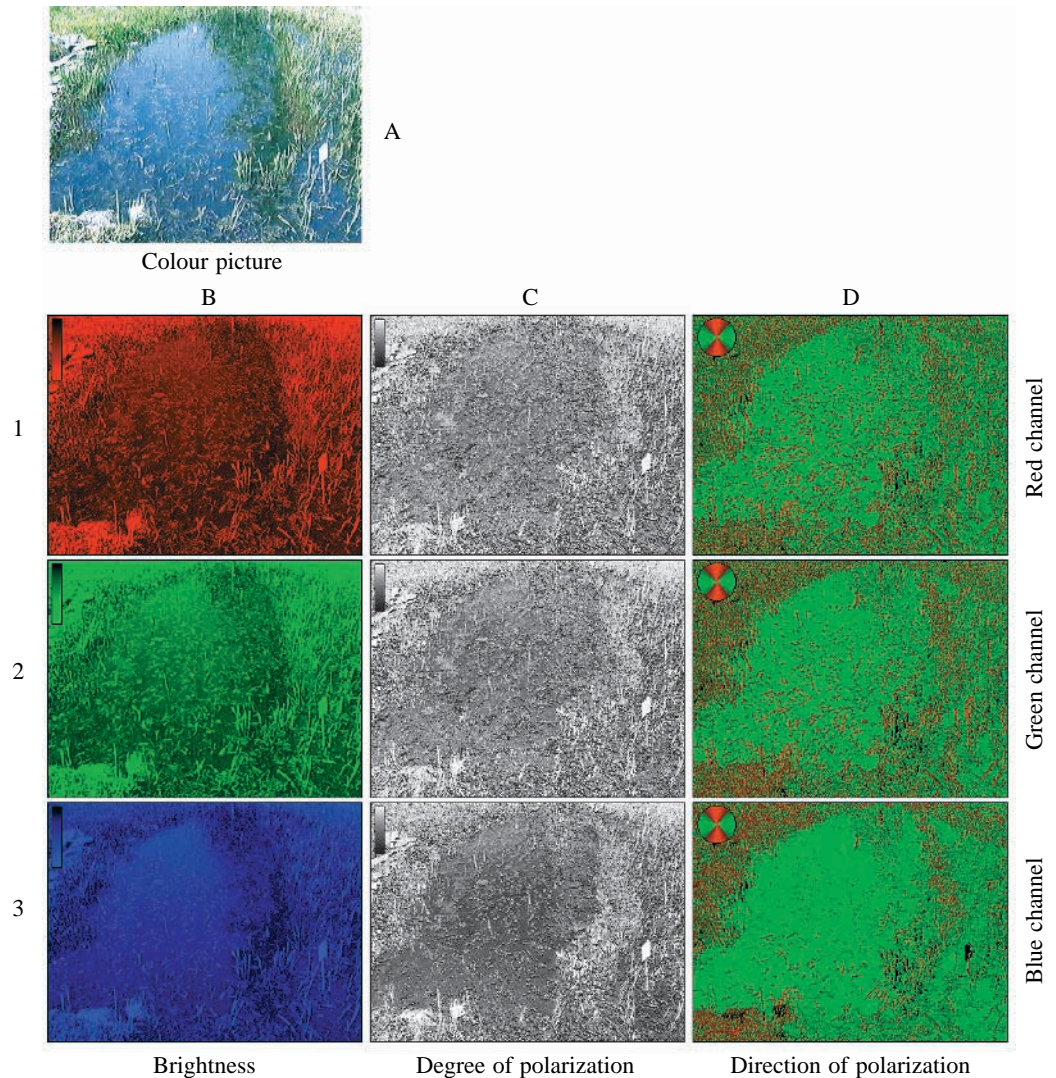


Fig. 3. (A) Colour picture of a small dark pond with clear water and a dense growth of aquatic plants under a clear sky on a sunny warm day. (B–D) Maps of the brightness (column B), degree of polarization (column C) and direction of polarization (column D) of the pond recorded through the red (row 1), green (row 2) and blue (row 3) channels of the camera. In column D, red represents more or less vertical and green more or less horizontal E-vector alignments, while black indicates unpolarized ( $\alpha=0\%$ ) light.

channel. In red and blue light, they are darker and the reflected light is more strongly polarized. The white fennel (or the violet eggplant) appears almost uniformly bright (or dark) and unpolarized (or highly polarized) in all three channels. From Fig. 2, we can conclude that the darker an object is in a given channel, the higher its degree of polarization. This holds as a general rule and is explained in the Discussion.

Using video polarimetry, we recorded in the field and then visualized the polarization patterns of freshwater habitats in different spectral ranges accessible to our video camera. Figs 3–6 represent the polarization patterns of two small ponds of different types recorded in the botanic garden of the University of Tübingen from an angle of view of  $50^\circ$  with respect to the vertical at the end of April 1996 on a sunny, warm day under a clear sky. Column B in Fig. 3 represents brightness maps for a dark pond with clear water and a dense growth of aquatic plants. In the red range, the water reflects only a small amount of light, unlike the plants in and around it. In the green range, the amount of surface-reflected light

from the sky is slightly larger, and in the blue range it dominates the picture so that the pond appears quite bright. The reason for this is that the incident light from the sky is predominantly blue. Column C in Fig. 3 maps the degree of polarization of the pond. In the red and green ranges, the water surface is less polarized than in the blue range. This is especially true at and near the Brewster angle ( $47.5^\circ$  from the vertical), where a dark patch appears in the centre of Fig. 3C3. The maps of the reflected E-vector indicate that, viewed through the blue channel, the surface of the pond reflects horizontally polarized light. The light reflected from plants in the water and from the grassy surroundings of the pond is approximately vertically polarized. In the red and green ranges of the spectrum, however, the contribution of the more or less vertically polarized light to the overall polarization of the pond is somewhat enhanced (Fig. 3D1,2).

The histograms in Fig. 4 show the distribution of the direction and degree of polarization in the red, green and blue ranges of the spectrum calculated for the central region

of the dark pond in Fig. 3. In the blue range, the most frequent values of the degree of polarization are concentrated around 60 %, while in both the red and green ranges these values are approximately 40 % (row 3 in Fig. 4). In all three spectral regions, the most frequent E-vector alignments are between 90° and 100° from the vertical (row 2 in Fig. 4); that is, the reflected E-vectors are concentrated about the horizontal direction. The small shift (<10°) of the peak of the E-vector histograms to the right can be explained by the fact that the incident light from the sky was partially polarized with different directions of polarization; thus, the reflected E-vectors are not always horizontal (see Schwind and Horváth, 1993; Horváth, 1995). However, in the blue range, the reflected E-vectors are more narrowly distributed around the main peak than in both the red and the green range.

In Fig. 5B,C,D, the same patterns as in Fig. 3B,C,D can be seen for the bright pond shown in Fig. 5A. Here, the pond was directly illuminated by sunlight, its left-hand side was in the shadow of a bush, and blue light from the sky was reflected from the right-hand side of the water surface. The water was clear and transparent, and its yellowish-green bottom reflected a relatively high proportion of light. In the red and especially in the green range of the spectrum, the shadowed bottom of the pond appears brighter than in the blue range (column B in Fig. 5). In the red and green ranges, the whole pond appears

only slightly polarized and is very similar to its grassy surroundings (Fig. 5C1,2). Only in the blue range and only in the skylight-reflecting region of the surface is the reflected light highly polarized (Fig. 5C3). The E-vector of light emanating from the water is more or less vertical in the shadowed area and horizontal where skylight is reflected from the water surface (column D in Fig. 5).

This is illustrated quantitatively in Fig. 6. In the blue range, the histogram of the degree of polarization has two peaks (Fig. 6C3): one at approximately 10 % and the other at approximately 38 %. The peak at 10 % is the contribution of the shadowed left-hand side of the pond, and the peak at 38 % originates from the right-hand side which is reflecting blue skylight. In the green range, these two peaks virtually coincide between 8 and 12 % (Fig. 6B3), and in the red range there is a single peak at approximately 10 %, because the difference in the degree of polarization between the left- and right-hand sides of the pond gradually disappears at longer wavelengths. In all the red, green and blue regions, the most frequent E-vector alignments are concentrated around 105° from the vertical (row 2 in Fig. 6). The reason for the shift of the peak by approximately 15° to the right in the E-vector histograms is the same as in the former example (Fig. 4). Here again, in the red and green ranges, the reflected E-vectors are more widely distributed around the main peak than in the blue range.

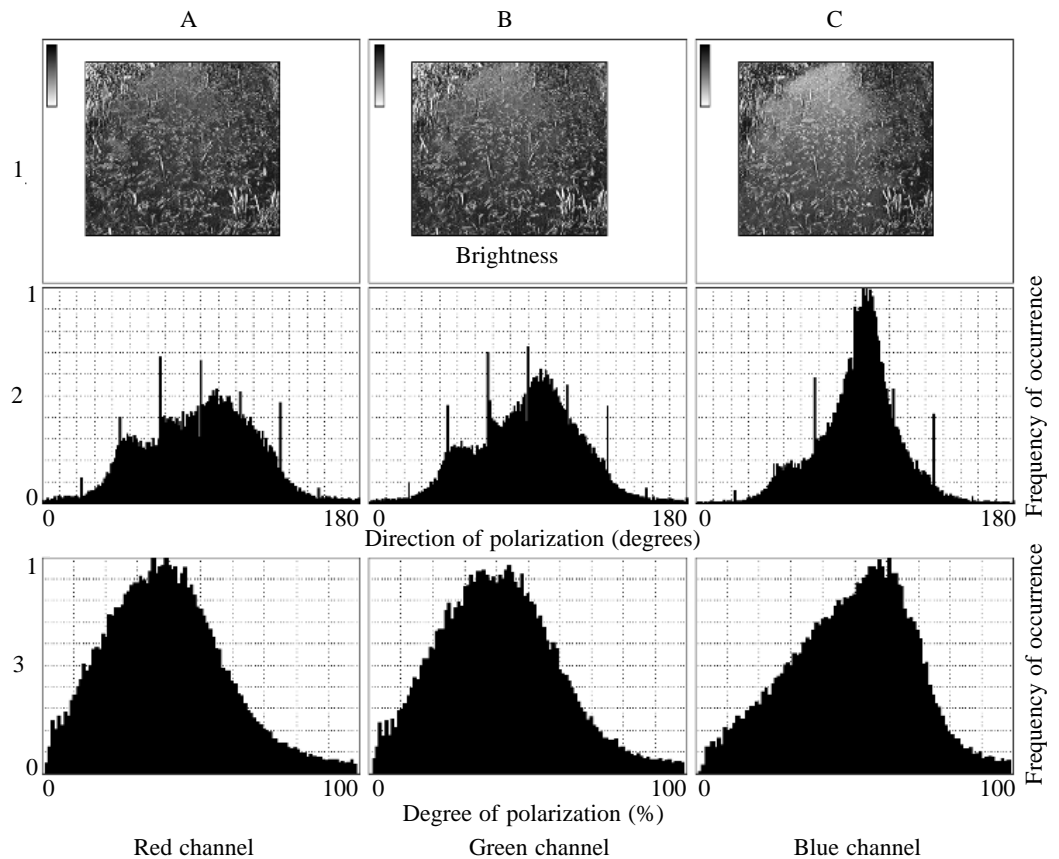


Fig. 4. The grey coded brightness map (row 1) and histograms of the distribution of the direction of polarization (row 2) and the degree of polarization (row 3) in the red (column A), green (column B) and blue (column C) ranges of the spectrum calculated for the central region of the dark pond in Fig. 3.

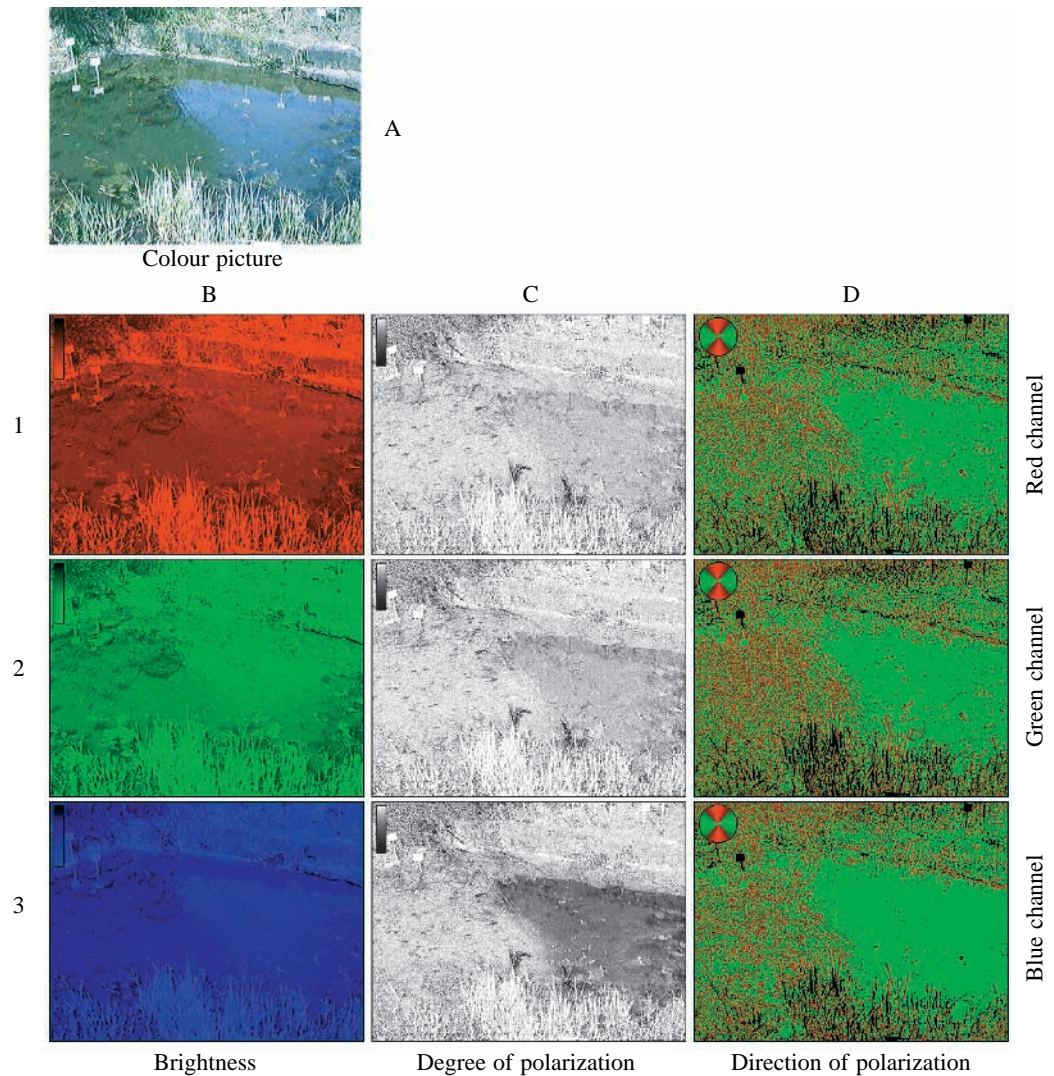


Fig. 5. As Fig. 3 for another pond, which is directly illuminated by sunlight, with its left-hand side in the shadow of a bush and with blue skylight reflected from the right-hand side of the water surface. The water is clear and transparent, and the yellowish-green bottom of the pond reflects a relatively large amount of light.

### Discussion

#### *Why use video polarimetry?*

Conventional polarimeters, used for instance in physics, chemistry, astronomy, engineering and industry for a variety of optical measurements (e.g. Azzam and Bashara, 1989; Collett, 1994), would be of little use in the analysis of natural scenes and to give insight into the information content of the visual world of animals. Using these polarimeters, it is possible to determine with a high degree of accuracy the optical parameters – brightness, degree and direction of polarization – of a light beam coming from a given direction. They cannot mimic, however, one of the fundamental features of the animal eye, the ability to receive instantaneous visual information from a wide field of view. While the polarization pattern of a visual environment could be determined by scanning the area with a conventional polarimeter, this would be a troublesome and time-consuming task which could only be performed in the laboratory using complicated, computer-controlled procedures. It is, therefore, not surprising that so far no biologists have used this technique.

In the last few years, French (Deschamps *et al.* 1994),

American (Wolff, 1993; Cronin *et al.* 1994; Shashar *et al.* 1995) and Hungarian-German (Horváth and Zeil, 1996) research teams have independently developed different techniques to measure and analyse polarized light in a wide field of view for different scientific purposes. These novel techniques are still relatively young and their use is not yet widespread. The French POLDER (POLARization and Directionality of the Earth's Reflectance) instrument is a radiometer to measure the directionality and polarization of the sunlight scattered by the ground and the atmosphere (Deschamps *et al.* 1994). This polarimeter with a wide field of view has been designed for installation in aircraft and satellites, and is not accessible to biologists. They can utilize, however, the polarization camera technology developed recently by Wolff (1993). This patented and copyrighted design includes two twisted nematic liquid crystals and a fixed polarizing filter in series in front of a CCD camera. There are two different configurations (Cronin *et al.* 1994; Shashar *et al.* 1995): an autonomous sensor (with an electronic box) that uses a camcorder for recording images that are analyzed at a later stage, and an on-line sensor that uses a digital camera

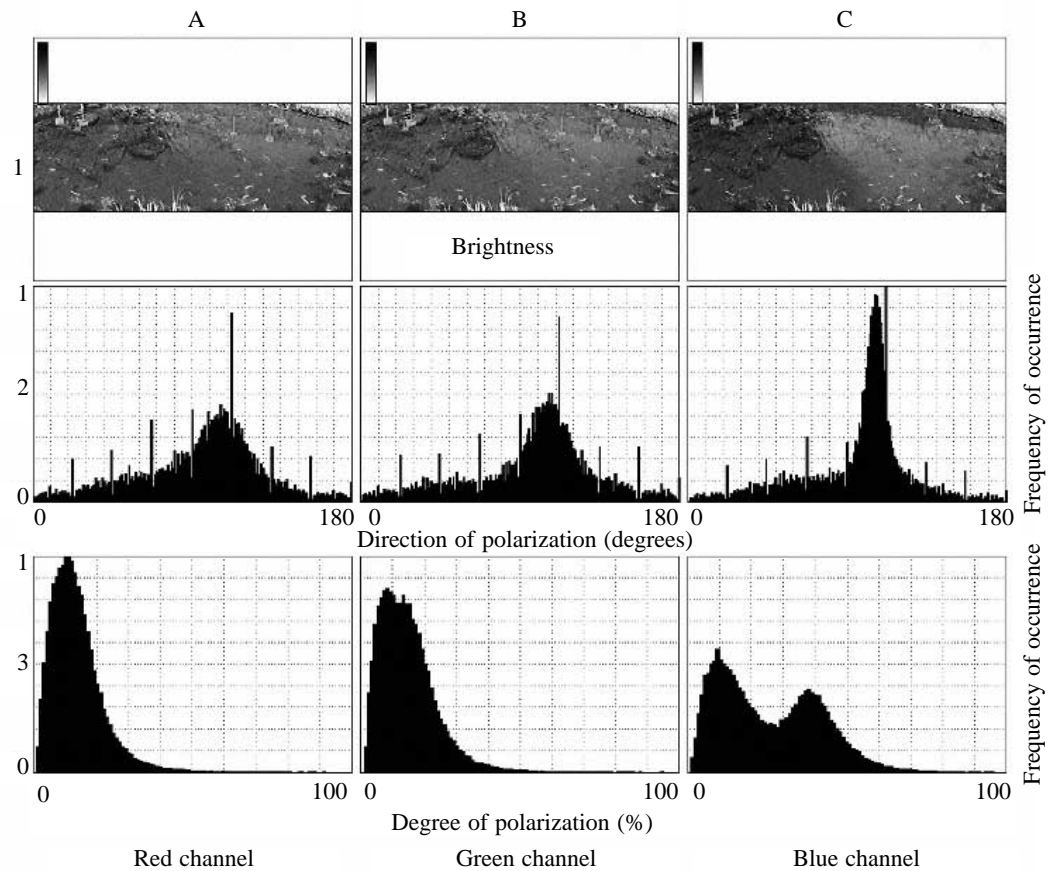


Fig. 6. The grey coded brightness map (row 1) and histograms of the distribution of the direction of polarization (row 2) and the degree of polarization (row 3) in the red (column A), green (column B) and blue (column C) ranges of the spectrum calculated for the central region of the pond in Fig. 5.

connected to a personal computer which controls and analyses the information. The third design, used by Horváth and Zeil (1996) and described in detail in this work, is a modest and low-cost apparatus that can be assembled by the user.

#### *Advantages and disadvantages of a rotating-analyzer video polarimeter*

The main advantage of the technique described in this work lies in its simplicity: one needs a rotating polarizer, a video camera recorder, a tripod, a personal computer and a frame grabber. Today all these items are commonly accessible for researchers. The recording takes place in the field and is separated from the evaluation and visualization of the polarization patterns in the laboratory. The computer programs evaluating and visualizing the recorded polarization patterns are written in program language C and can, with a little effort, be developed and improved.

The simplicity of the design, however, also results in some disadvantages. The rotation of the polarizer and the acoustic coding of its direction require a few seconds. During this time, the recorded object must not be displaced. Any rotation or translation of the target, which can be brought about by wind or motion, results in 'motion artefacts' in the map of polarization, because it is almost impossible to distinguish the intensity modulation due to polarization from that caused by

motion. Hence, this technique can be used in the field only for recording the polarization patterns of motionless objects in biotopes or landscapes under still conditions.

It is important that the polarizing filter is of high optical quality, otherwise the imaging will be poor and the results questionable. Since the polarization ellipse can be characterized by three parameters (major axis, minor axis, alignment of the major axis), it is sufficient to carry out recordings with the polarizer turned in three different directions. These directions can be arbitrary, but they should be well-separated from each other; for example  $\phi$  can be  $0^\circ$ ,  $45^\circ$  and  $90^\circ$  (our preferred set of angles) or  $0^\circ$ ,  $60^\circ$  and  $120^\circ$ . We tested our method by taking pictures and changing the direction in 10 steps each of  $15^\circ$ . When the results were statistically compared with those in which three much larger step changes had been made, no significant differences were found.

The totally polarized light transmitted by the polarizer is refracted and reflected by lenses and prisms in the camera. This results in inevitable minor changes to the original polarization pattern. This camera artefact, however, affects both the degree and direction of polarization by only approximately 1%, which is tolerable in biological applications.

A further problem is the saturation of the CCDs of the camera: beyond a certain light intensity, the detector array

becomes unresponsive to further intensity changes. The highly polarized regions of an object are normally associated with its shiny parts, which reflect a large amount of light, and it is in these areas of the digitized video picture where the CCDs can become saturated. During recording, such saturation can be avoided by the use of different neutral density filters and suitably selected smaller gains, shutter speeds or apertures, which reduce the amount of light received by the detector array.

#### *Polarization and colour*

The reflection-polarization patterns of colourless objects (matt or shiny) are independent of the wavelength of light. This is, however, not true in the case of shiny coloured objects with a smooth surface such as the fruits and vegetables in Fig. 2. These vegetables have a smooth skin, which reflects light efficiently. The mirrored light is more or less partially polarized depending on the incident angle, but almost independently of the wavelength, and its E-vector is always parallel to the surface.

The colour of these vegetables stems from the selective absorption and diffuse scattering of light in the tissue below their transparent skin. The diffuse light emanating from the tissue is originally unpolarized, but it becomes partially polarized after transmission and refraction at the skin. The E-vector of the tissue-scattered light is always perpendicular to the skin because of refraction polarization (Horváth and Varjú, 1995). Hence, the net degree and direction of polarization of a vegetable are determined by the superposition of the surface-reflected and the subsurface-scattered light. If the former dominates, then the direction of polarization is parallel to the surface; otherwise, the E-vector is perpendicular to it. In these spectral regions where the subsurface-scattered light makes a considerable contribution to the net polarization, the degree of polarization of the mirrored light is reduced or even abolished.

This is the case, for example, for the reddish fruits and vegetables seen through the red channel in Fig. 2. In the green and blue spectral regions, the amount of light emanating from the reddish tissue is low in comparison with the surface-reflected light; thus, the degree of polarization is enhanced when viewing these objects through the green and blue channels. The absence, or the considerably reduced amount, of subsurface-scattered light in the green and blue channels causes the reddish objects to be dark. This is the physical reason for the general rule that in a given spectral region the darker objects polarise light to a higher degree if the illuminating light is unpolarized and white.

#### *Reflection-polarization pattern of small bodies of water and its relevance for the habitat choice of aquatic insects*

What we have learnt from the reflection polarization of coloured fruits and vegetables (Fig. 2) can also be applied to small freshwater habitats. The light reflected from the water surface is more or less horizontally polarized depending on the angle of view and on the illumination conditions (sunlight or light from a clear or overcast sky; see Horváth, 1995). In

contrast, light coming from water and refracted at the water-air interface is always vertically polarized (Horváth and Varjú, 1995). Thus, the direction of polarization depends upon the balance between these two light components. If the former dominates, then the direction of polarization is horizontal, while if the latter dominates, the E-vector is vertical. If the contribution of both is about the same, the net degree of polarization is considerably reduced.

Only a small amount of vertically polarized light is returned in all three spectral ranges from the dark pond in Fig. 3. In the red and green ranges, this vertical polarization is slightly overcompensated by the horizontal polarization of the reflected skylight, the intensity of which is, however, much higher in the blue than in the red or green range, because it contains a predominantly blue component. Thus, the degree of polarization is low in the red and green ranges and high in the blue, especially at and near the Brewster angle (Figs 3, 4).

This effect is stronger in the case of the bright-bottomed pond in Fig. 5, in the right-hand part of which the reflected blue skylight dominates all three spectral ranges; thus, the E-vector is horizontal (column D in Fig. 5). In contrast, owing to the shadow, the amount of light reflected from the left-hand side of the water surface is much lower, and the light returning from the subsurface region dominates in all three spectral ranges. Thus, the direction of polarization on the left-hand side of the pond is vertical (column D in Fig. 5). In the red and green ranges, the net degree of polarization is small (Figs 5C1,2, 6A3,B3), because the horizontally polarized surface-reflected light is almost totally compensated by the vertically polarized refracted light from the subsurface region.

Interestingly, the crude oil lakes in Kuwait and the Pleistocene tar seeps in Rancho La Brea and Starunia are more attractive to aquatic insects than natural waters because of the above-mentioned phenomena (Horváth and Zeil, 1996).

We were not able to perform video polarimetric measurements in the ultraviolet range of the spectrum but, as Schwind (1985, 1991, 1995) pointed out, in this spectral region the contribution of surface-reflected light to the net polarization is much stronger, because the bottom and the water body itself return almost no ultraviolet light.

These reflection-polarization characteristics of small freshwater habitats are in accordance with the earlier results of Schwind (1995), who found that in eutrophic habitats the degree of polarization is highest in the ultraviolet region and gradually decreases towards the long-wavelength end of the spectrum, and that in dark water bodies the light at long wavelengths can be highly polarized (see Fig. 8A in Schwind, 1995). This is of great importance for water-seeking insects, which rely on highly horizontally polarized light during their habitat selection, and thus are not attracted by bodies of water which reflect vertically polarized light or horizontally polarized light with a low degree of polarization. Schwind (1991, 1995) demonstrated that the polarization-sensitive water-detecting system (POL system) of several aquatic insects operates in the short-wavelength (ultraviolet or blue) region of the spectrum, which is an adaptation to the high degree of



polarization of reflected light in this spectral range. The POL system of other aquatic insects, however, operates in the long-wavelength regions, and might be adapted to the spectral characteristics of the underwater visual environment.

The financial support of the Hungarian State Eötvös Scholarship Fund (MÖB) and the National Scientific Research Foundation (OTKA F-014923 and OTKA T-020931) to G.H. and a grant from the Deutsche Forschungsgemeinschaft to D.V. (SFB 307) are gratefully acknowledged. We are grateful to H.-J. Dahmen and H. Ritter for their technical assistance, advice and support.

### References

- AZZAM, R. M. A. AND BASHARA, N. M. (1989). *Ellipsometry and Polarized Light*. Amsterdam, New York: North-Holland
- COLLETT, E. (1994). *Polarized Light. Fundamentals and Applications*. New York: M. Dekker Inc.
- CRONIN, T. W., SHASHAR, N. AND WOLFF, L. B. (1994). Portable imaging polarimeters. *Proceedings of the 12th IAPR International Conference on Pattern Recognition*. pp. 606–609.
- DESCHAMPS, P. Y., BRÉON, F. M., LEROY, M., PODAIRE, A., BRICAUD, A., BURIEZ, J. C. AND SÉZE, G. (1994). The POLDER mission: Instrument characteristics and scientific objectives. *IEEE Trans. Geosci. Rem. Sens.* **32**, 598–615.
- HORVÁTH, G. (1995). Reflection-polarization patterns at flatwater surfaces and their relevance for insect polarization vision. *J. theor. Biol.* **175**, 27–37.
- HORVÁTH, G. AND VARJÚ, D. (1995). Underwater refraction-polarization patterns of skylight perceived by aquatic animals through Snell's window of the flat water surface. *Vision Res.* **35**, 1651–1666.
- HORVÁTH, G. AND ZEIL, J. (1996). Kuwait oil lakes as insect traps. *Nature* **379**, 303–304.
- SCHWIND, R. (1985). Sehen unter und über Wasser, Sehen von Wasser: das Sehsystem eines Wasserinsektes. *Naturwissenschaften* **7**, 343–352.
- SCHWIND, R. (1991). Polarization vision in aquatic insects and insects living on a moist substrate. *J. comp. Physiol. A* **169**, 531–540.
- SCHWIND, R. (1995). Spectral regions in which aquatic insects see reflected polarized light. *J. comp. Physiol. A* **177**, 439–448.
- SCHWIND, R. AND HORVÁTH, G. (1993). Reflection-polarization pattern at water surfaces and correction of a common representation of the polarization pattern of the sky. *Naturwissenschaften* **80**, 82–83.
- SHASHAR, N., CRONIN, T. W., JOHNSON, G. AND WOLFF, L. B. (1995). Portable imaging polarized light analyzer. *SPIE Proc. Series* **2426**, 28–35.
- WOLFF, L. B. (1993). Polarization camera technology. *Proc. DARPA Image Understanding Works*. pp. 1031–1036.